

Direct measurement of indentation frame compliance

Krystyn J. Van Vliet

Department of Surgical Research, The Children's Hospital and Harvard Medical School, Boston, Massachusetts 02115

Lubos Prchlik

Department of Materials Science and Engineering, Massachusetts Institute of Technology, Cambridge, Massachusetts 02139

James F. Smith

MicroMaterials Limited, Unit 3, Wrexham Technology Park, Wrexham LL13 7YP, United Kingdom

(Received 16 June 2003; accepted 13 October 2003)

Accurate determination of frame compliance is an essential component of instrumented micro- and nanoindentation experiments. In load frames of finite stiffness, the load applied via the indenter induces displacement in both the sample and the load frame. Frame compliance must be identified and subtracted from the total indenter displacement to account properly for sample deformation. Current experimental procedures, in which the frame compliance is inferred from the elastic unloading indentation response of a reference sample, are based on several assumptions and simplifications that can propagate significant uncertainty with respect to subsequent analyses of mechanical behavior of the sample. We outline a new procedure that measures the compliance of the load frame, and identify the effects of load, loading direction, and loading rate on the measured compliance, as well as several possible sources of uncertainty in other available methods of frame compliance determination.

I. INTRODUCTION

Recent developments in the analysis of instrumented or depth-sensing indentation present the opportunity to quantify both the elastic and plastic mechanical properties of materials, including elastic modulus E , yield strength σ_y , and strain hardening exponent n .¹⁻⁴ The calculation of plastic mechanical properties requires that indentation data are obtained with accuracy and precision greater than that required for determination of only elastic properties.^{3,5,6} The accuracy of the indentation load-displacement ($P-h$) response is defined by the calibration of three factors: load P , displacement h , and load frame compliance C_f . Although the calibration of C_f , a measure of the load frame displacement incurred per unit applied load, is as crucial to the accuracy of the data as the basic force and displacement transducer calibrations, its proper implementation has received relatively little attention. Indentation instruments are designed to minimize this compliance, and most manufacturers estimate the magnitude of C_f according to the method of Oliver and Pharr¹ and modifications thereof. Commercial instruments exhibit C_f in the range of 10^{-5} to 10^{-7} m/N, which means that the instrument displaces as much as 10 nm for a maximum applied load P_{\max} of 10 mN in nanoindentation experiments (the equivalent of 10 μm displacement for $P_{\max} =$

10 N during microindentation). Such displacements comprise a significant fraction of indentation depth for many natural and engineered materials currently studied via indentation.

The level of accuracy attained in the calibration of C_f significantly affects the quantitative interpretation of the $P-h$ response. Because frame compliance is affected by any changes in the stiffness of load frame components, this value should be established precisely and accurately whenever the load train is modified mechanically. Even when indentation data are not utilized for mechanical property extraction, but rather for qualitative comparison, proper determination of C_f is critical in order for results to be compared over time and among groups. Furthermore, inaccurate determination of C_f can skew qualitative results sufficiently to cause gross misinterpretation of even qualitative data.

Methods exist in the literature to infer C_f via extrapolation of indentation experimental data which involve either the estimation of the maximum indentation contact area A_{\max} ^{1,2} or the optical measurement of the residual indentation contact area A_{res} in relatively soft reference samples.⁷ Inherent to each of these indirect determinations of C_f are simplifying assumptions regarding the elastoplastic indentation response of the sample (e.g., the assumption that hardness is constant with h) and the me-

chanical response of the load frame. Here, we briefly review these existing methods and propose a new method for direct measurement of C_f .

II. METHODOLOGY REVIEW

To appreciate the strengths and weaknesses of the various approaches, we shall discuss the details and inherent assumptions of alternative, indirect estimations of C_f . Doerner and Nix were the first to propose a method whereby elastic modulus E and hardness p_{avg} of a material could be established solely from the P - h response,⁴ rather than from a post-test, optical measurement of A_{res} , where

$$P_{\text{avg}} = P_{\text{max}}/A_{\text{max}} \quad (1)$$

Here, the authors assumed that the total compliance C_{TOT} measured in the experimental P - h response was the sum of the sample compliance C_s and frame compliance C_f in series

$$C_{\text{TOT}} = C_s + C_f \quad , \quad (2)$$

such that the reduced elastic modulus of the sample E_r is related according to Sneddon's elastic punch solution

$$C_{\text{TOT}} = dh/dP|_s + C_f = (1/2E_r)(\pi/A_{\text{max}})^{0.5} + C_f \quad , \quad (3)$$

where $dh/dP|_s$ is a numerical (here, linear) fit to the experimentally measured, initial unloading compliance of the sample and is equivalent to $1/S$, where S is stiffness or $dP/dh|_s$. The value of A_{max} is calculated for an idealized sharp (Vickers) indenter as

$$A_{\text{max}} = 24.5h_p^2 \quad , \quad (4)$$

where h_p is the plastic depth of indentation, a value extrapolated from the linear fit to the initial unloading response down to zero load rather than measured experimentally. Substituting Eq. (4) into Eq. (3) provides a linear relationship between sample compliance $dh/dP|_s$ and h_p

$$dh/dP|_s = 0.179/E_r(1/h_p) \quad . \quad (5)$$

Thus, a set of experiments to different ($P_{\text{max}}, h_{\text{max}}$) in a single sample for which E_r is independent of h_{max} results in a linear function that can be extrapolated to $h_p = \infty$ to obtain an indirect estimate of C_f . That is, any displacement not resulting from sample deformation is attributed to displacement of the load frame. In this manner, Doerner and Nix inferred a frame compliance of 3×10^{-7} m/N, additional to that estimated for springs within the load train and due presumably to the deflection of other load train components (e.g., sample mounting, stage bearings). The authors asserted that this contribution to

C_f could not be calibrated directly, only inferred post-test.

Oliver and Pharr subsequently presented an improved methodology for calibrating C_f and the diamond area function $A(h_c)$, a mathematical representation of the deviation from ideal indenter geometry.¹ In its more mathematically intensive (and less frequently used) embodiment, the Oliver-Pharr method requires iterative calculation of C_f and $A(h_c)$: As in the Doerner-Nix approach, a set of experiments are conducted and a plot of C_{TOT} versus $A_{\text{max}, 1}^{-1/2}$ is constructed, where

$$y = mx + b = \pi^{-1/2}/(2E_r)x + C_f \quad , \quad (6)$$

and Eq. (4) defines an ideal $A_{\text{max}, 1}(h_c)$, or the estimation of A_{max} based on an idealized indenter geometry and material response. With the values of E_r and C_f thus obtained, a second, theoretically equivalent, estimate of A_{max} is calculated based on Eq. (3)

$$A_{\text{max}, 2} = (\pi/4)(1/E_r^2)(C_{\text{TOT}} - C_f)^{-2} \quad . \quad (7)$$

It is assumed that discrepancy between $A_{\text{max}, 1}$ and $A_{\text{max}, 2}$ is due to geometric imperfections of the indenter (tip bluntness, imprecision in the apex angle). Thus, Eq. (4) is modified to express $A(h_c)$ as a polynomial of decreasing powers of h_c (the so-called diamond area function), and this process is iterated until the values of C_f , E_r and A_{max} converge.

Note that h_c is not an experimentally measured quantity, but rather is calculated by assuming two features of deformation: (i) that h_c is less than the total measured maximum depth h_{max} due to sinking-in of the material immediately adjacent to the indenter; and (ii) that this sink-in depth h_s can be quantified semiempirically as

$$(h - h_c) = h_s = \epsilon P_{\text{max}} dh/dP|_s \quad , \quad (8)$$

where ϵ is a function of indenter geometry which is empirically determined. The above approach not only introduces any uncertainty associated with the estimation of ϵ or calculation of $dh/dP|_s$ from the unloading data, but also requires that the indented material sink in. This is a difficult requirement to meet, in that accurate calibration over an appreciable range of load and displacement accessed via microindentation ($h_{\text{max}} > 500$ nm) requires the utilization of soft metal that may strain harden readily during processing and/or sample surface preparation. Such metals typically pile-up at the indentation perimeter, a discrepancy that would introduce significant uncertainty into the calculation of h_c and, by extension, any frame compliance or material parameters related to this quantity, a limitation discussed by Pharr et al.^{8,9}

To address this effect of pile-up (and sink-in) on the estimation of A_{max} and C_f , McElhaney et al.⁷ conducted a thorough and experimentally intensive investigation whereby indentations were imaged via scanning electron

microscopy, and A_{res} was measured precisely from these images. By plotting dh/dP versus $A_{\text{res}}^{-0.5}$, C_f was obtained as the intercept. Implicit in this analysis is the assumption that minimal elastic recovery occurred during unloading, such that A_{res} is approximately equal to A_{max} , and was verified indirectly via calculation of E for the indented samples that agreed well with calculated values obtained by the same group and the same instrument when using the Oliver–Pharr method of C_f determination.¹⁰ In addition, as this method requires extrapolation to infinite A_{res} ($C_s = 0$), the accuracy of this approach is also limited by both the assumption of linearity near $C_s = 0$ and by the maximum indentation size, a feature constrained by the maximum loads and depths achievable for the particular instrument. These and other contributions to uncertainty in C_f calculation are shown in Table I. Importantly, the above methods rely strongly on the unloading indentation response to calculate C_f and consider the loading response only insofar as these data terminate at h_{max} and thus affect extrapolation of h_p or h_c . As such, features of frame compliance restricted to the loading portion of the indentation cycle are not realized and make the implicit, uncorroborated assumption that C_f is not a function of load or loading rate. Moreover, standard implementations of these procedures propagate uncertainty in C_f determination, either via coupling of this value with other material and machine calculations or making implicit assumptions about material behavior under indentation.

III. PROPOSED METHODOLOGY FOR DIRECT MEASUREMENT OF C_f

Here, we propose direct measurement of C_f to eliminate both mathematical uncertainties due to analytical formulations and assumptions regarding material and machine behavior. The indenter holder/indenter assembly in the load train is replaced with an identical indenter holder to which no indenter has been attached, such that the sample will be loaded with a flat punch (platen) of diameter of the order several millimeters. The platen is

mounted to the load train via a pin-nut arrangement [Fig. 1(a)], such that the platen can be removed from the load train without imposing significant torque. The contact face of the platen and the stage-mounted sample are ground and polished flat. Ideally, these mating components are machined from the same base material, and the final polishing step is the displacement of fine-grit paper between the mounted platen and stage-mounted sample to ensure precise parallelism between the mating faces. The surfaces are then cleaned with acetone and dried, and the punch is coated with a thin film of low viscosity (<5 cP) cyanoacrylate or a similar thermoplastic adhesive. (The viscosity of the adhesive must be low to minimize the final layer thickness. For viscosity <5 cP, the *maximum* gap fill is approximately 50 μm .) The platen is then positioned into firm contact with the sample holder via instrumentation software (e.g., stage displacement toward a fixed indenter position) and held under load $P > 10$ N to minimize layer thickness until the cyanoacrylate is fully polymerized (>1.5 h). A loading cycle is applied, and the load and the depth are measured continuously, just as in a standard indentation experiment. The loading profile can be modified in terms of loading rate dP/dt , P_{max} , and dwell time at P_{max} without removing the platen from contact with the sample stage, until an appropriate range of these variables is tested. For each loading cycle, a line is fit to both the loading and unloading data; the slope of each line represents the direct measurement of C_f for the corresponding loading direction. When measurements for a desired range of operating parameters are complete, the platen is decoupled from the load train via the pin-nut mount, the stage is retracted from the load train, and the platen and sample/stage (now bonded together) are removed from the stage.

We found that the parallel polishing and cyanoacrylate layer were necessary to ensure (i) that asperities and air gaps did not contribute to the measured response and (ii) that the platen displaced normal to the sample surface, eliminating initial contact at the platen periphery. Repeatability from measurement to measurement was poor in the absence of cyanoacrylate bonding. As the contact

TABLE I. Contributions to error propagation in estimation of C_f .

Step in C_f calculation	Source of uncertainty
Throughout	Implicit assumption of accuracy in Eqs. (2) and (3): C_f inferred, not measured directly
Throughout	Restriction of analysis to unloading data
Determination of $A(h)$ via Eq. (4) or polynomial expansion	Assumes geometric perfection of indenter
Determination of $A(h)$ through polynomial expansion/iteration of Eq. (4)	Assumes material sink-in
Iteration of Eqs. (6) and (7)	Inaccurate calculations of A_{max} (h_c) and E_r propagate
Empirical determination of h_c in Eq. (8)	Assumes material sink-in and value of ϵ
Calculation of dh/dP for use in Eqs. (3), (5), and (8)	Assumes functional form of unloading response (e.g., power law) and depends strongly on the portion of unloading response selected for fitting
Determination of A_{max} via visual inspection	Standard image analysis/resolution uncertainties

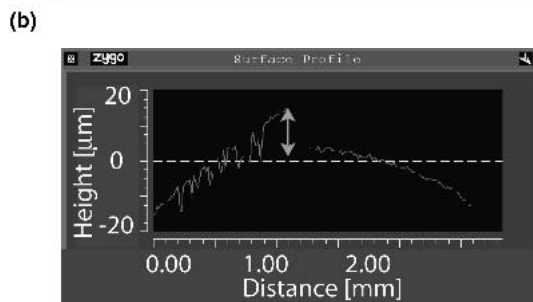
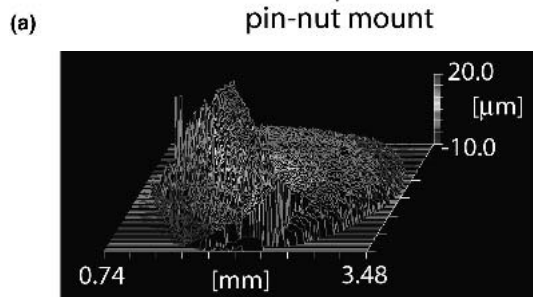
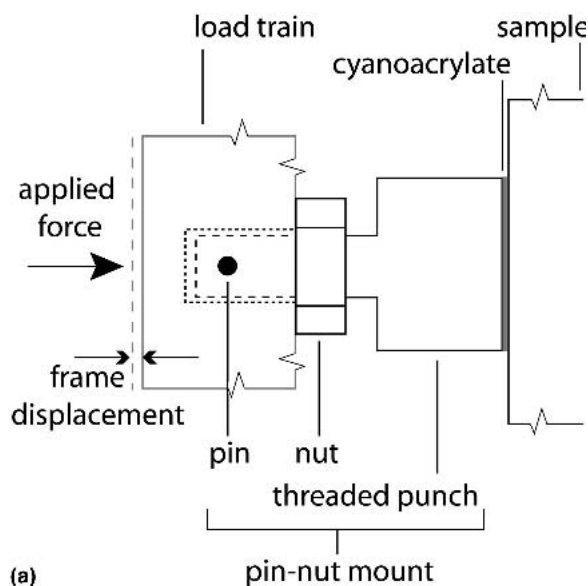


FIG. 1. (a) Schematic detailing flat punch mount used in direct frame compliance determination. The through-pin secures the punch when the nut is tightened against the threaded post. After testing is complete, the nut is loosened manually and the pin is removed to allow full retraction of the bonded punch-sample without damage to the load train. Noncontact 3D optical profilometry (Zygo, Middlefield, CT), (b) oblique view, and (c) surface profile of flat punch surface after debonding indicates a cyanoacrylate layer thickness of approximately 10 μm .

area of the platen is orders of magnitude greater than that of the (e.g., conical) indenter itself, applied loads of the range used in indentation testing will impose only small, elastic stresses at the bonded interface. Thus, the displacement measured during contact will be due only to the compliance of the load frame.

To determine whether the cyanoacrylate layer may contribute significant additional compliance, we measured the final thickness of the layer via both noncontact

and contact profilometry and estimated the minimum elastic modulus of the layer E_L to be 4 GPa. [Although the elastic modulus E of cyanoacrylate is not measured or quantified by manufacturers, the mechanical behavior of the cured adhesive is quantitatively quite similar to an acrylic.¹¹ The shear modulus G of acrylic is 1.5 GPa and the Poisson's ratio ν is 0.33. If the acrylic is idealized as a time-independent, isotropic material, then $E = 2G(1 + \nu) = 4$ GPa.] Defining the compliance of the layer as

$$C_L = \Delta L/P = \epsilon L/P = L/EA \quad , \quad (9)$$

where L is cyanoacrylate layer thickness, ϵ is engineering strain, and A is the contact area between the flat indenter holder and the sample stage (πR^2). Noncontact laser profilometry of the layer on a ground punch indicated layer thickness $L = 10 \mu\text{m}$ [Figs. 1(b) and 1(c)]. Contact profilometry of the layer on a polished punch, in which the indenter was operated as a profilometer, indicated $L = 1.50 \pm 0.09 \mu\text{m}$. Clearly, the value of L can vary but will be $\ll 50 \mu\text{m}$ for low-viscosity cyanoacrylate that is polymerized under compression. For R of 1.5 mm (radius of the flat indenter holder) and an estimated L of 50 μm , we estimate the *maximum* additional compliance due to this cyanoacrylate layer to be $<0.002 \mu\text{m}/\text{N}$. To determine the finite compliance of the aluminum sample stage under localized compression via the flat indenter holder, finite element modeling (FEM) simulations were used, and a maximum contribution of $0.0005 \mu\text{m}/\text{N}$ was determined. Thus, the resolution of this approach is estimated to be the sum of these factors, or $\pm 0.002 \mu\text{m}/\text{N}$.

IV. RESULTS AND DISCUSSION

We conducted the above direct C_f calibration procedure on two instruments manufactured by the same company (Micro Materials Limited, Wrexham, U.K.), located at different sites and operated by different users. Here, we discuss the results for each instrument (hereafter denoted I1 and I2), including subsequent indentation analysis of well-characterized materials with sharp (Berkovich) diamond indenters.

The load train of this instrument comprises an electromagnetically actuated pendulum that is instrumented at the free end with a threaded, interchangeable indenter. This configuration results in a horizontal indentation loading axis that is normal to the sample surface [Fig. 1(a)] and in an indenter mount that allows removal of the indenter even when it is rigidly fixed to a sample surface. Load is measured via electromagnetic coil current, and depth is measured via a capacitor located behind the indenter, in which one plate is fixed and the other is attached to the indenter itself.

Figure 2 shows the values of C_f obtained for a range of P_{max} for I1. Clearly, the compliance measured by this

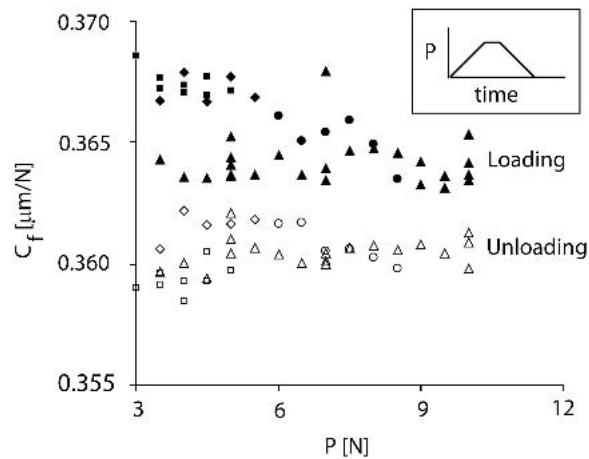


FIG. 2. Frame compliance as a function of maximum load via the direct method proposed in the text. These data were obtained on instrument I1 over the course of 1 year for several load train configurations. Each symbol represents a given load train configuration and test date: closed symbols indicate frame compliance in the loading direction, and open symbols indicate frame compliance in the unloading direction. Certain load train configurations show a weak, inverse dependence on load, though the average value of compliance measured over the course of this study did not vary more than the estimate of $\pm 0.002 \mu\text{m}/\text{N}$ due to uncertainties in compliance of the adhesive layer and stage material.

method indicates an effect of loading direction. If the load train were a perfect, linear spring, neither of these effects would be observed but, experimentally, C_f is consistently greater upon loading than upon unloading. Hereafter, we denote the directly measured frame compliance upon loading as C_f^L and upon unloading as C_f^U . The dependence of C_f on loading direction and on load depend strongly on the nature of the components within the load train and on the accuracy of the calibration relating load and depth to the measured output signal (e.g., volts). For both I1 and I2, we measured a remarkably repeatable and statistically significant difference between C_f^U and C_f^L : The value of C_f^U was of 1.4% less than that of C_f^L , regardless of maximum load P_{max} , loading rate dP/dt , or the presence of the adhesive layer, indicating a true loading dependence in the response of this particular load train. Certainly, this method does not indicate what component(s) of the load train cause this dependence on loading direction, but this approach is uniquely capable of identifying and quantifying this effect. As a result, the instrument load train can be analyzed to eliminate such an effect, and/or experimental loading and unloading data can be adjusted for frame compliance separately and more accurately. Loading rate was not observed to produce a statistically significant effect on the measured value of C_f : C_f^L decreased by 0.4% and C_f^U increased by 0.1% for a 125% increase in dP/dt —trends well within the standard deviation of our measurements.

Table II compares the value of C_f obtained for I1 using

TABLE II. Comparison of methods of C_f estimation.

Method	C_f ($\mu\text{m}/\text{N}$)
Direct	0.3514
Modified McElhane	0.3385
Modified Oliver–Pharr extrapolation	0.3105
Modified Oliver–Pharr inference	0.2624

Extrapolated and inferred data are for fused quartz.

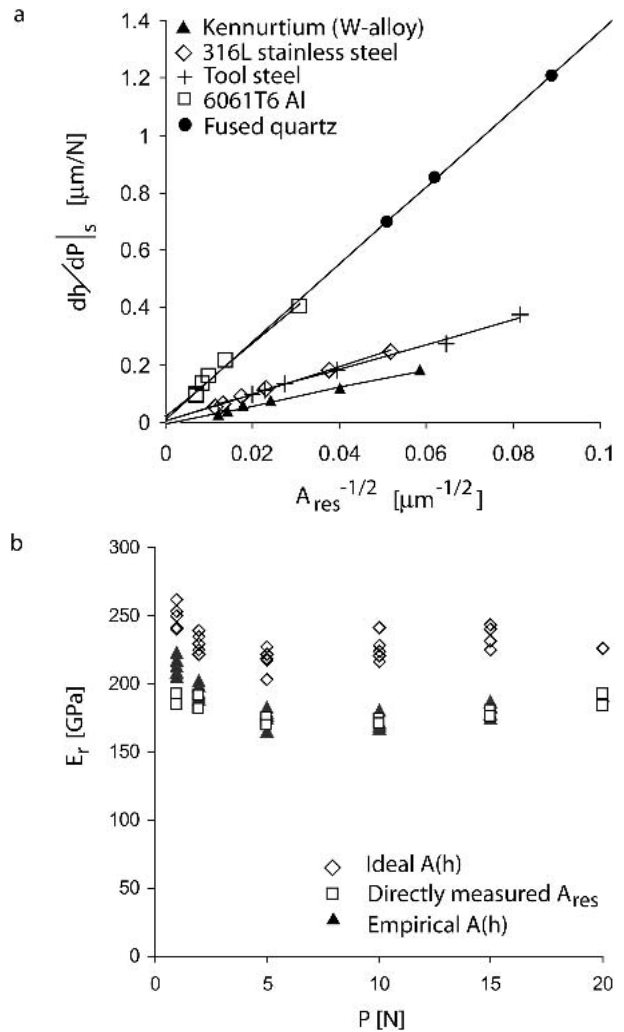


FIG. 3. (a) Sample compliance as a function of maximum contact area, as estimated via image analysis of the indentation after complete unloading. All data have been adjusted for the value of frame compliance determined via the direct method presented in the text. Extrapolation of these trends to a value identical to zero would indicate that the direct method accounts fully for compliance that is not due to sample deformation. In actuality, these data extrapolate to a nonzero, additional compliance of $\pm 0.009 \mu\text{m}/\text{N}$, as discussed in the text. (b) Contrast among values of E_f calculated for different estimates of A_{res} for 316L stainless steel. The empirical determination of $A(h)$ was a three-term polynomial expansion of the ideal area function for a Berkovich indenter, after adjusting each data set for the directly measured value of frame compliance.

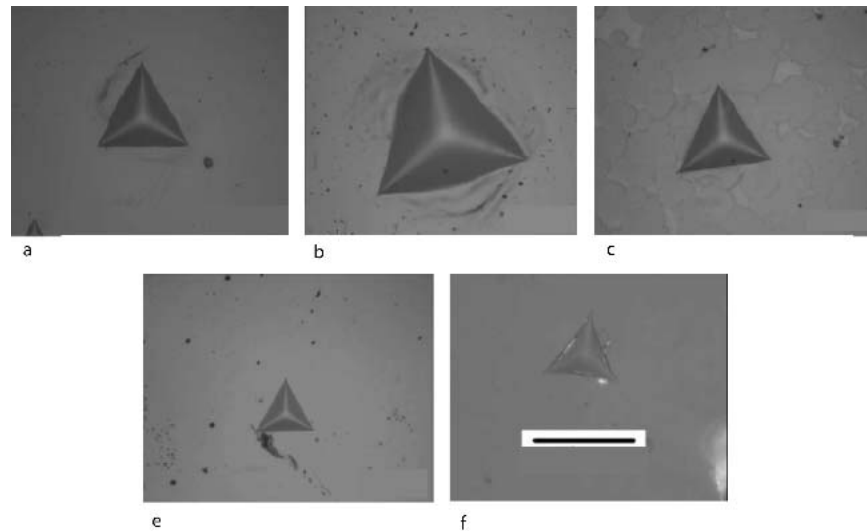


FIG. 4. Optical micrographs of Berkovich diamond indentations on various samples. Residual indentation contact area A_{res} was measured to calculate C_f according to the modified Oliver–Pharr extrapolation of C_f versus $A_{\text{res}}^{-0.5}$. (a) 316 stainless steel; (b) 6061T651 aluminum alloy; (c) kennurrium, a W-based alloy; (d) hardened tool steel; and (e) fused quartz. (a)–(d) at $P_{\text{max}} = 10 \text{ N}$; (e) at $P_{\text{max}} = 3 \text{ N}$. Scale bar = $50 \mu\text{m}$.

four methods: (i) direct measurement proposed herein; (ii) modified McElhaney: extrapolation via Eq. (6) where C_f is the intercept of experimentally measured C_{TOT} versus measured $A_{\text{res}}^{-1/2}$ for a series of indentations on a single material (fused quartz); (iii) modified Oliver–Pharr: extrapolation via Eq. (6) where $A_{\text{max}} = 24.5 h_c^2$; and (iv) common adaptation of Oliver–Pharr: inference of C_f by determining the value required for a material of known E_r and p_{avg} (fused quartz) according to Eqs. (1), (4), and (5). The observed variation in the value of C_f is a result of the artifacts of estimates discussed above. Note that simultaneous estimation of C_f and $A_{\text{max}}(h_c)$ can offset errors in the calculation of each parameter, such that the calculated values of E_r and p_{avg} may still agree well with independent measurements of these properties in a reference sample.

Figure 3(a) shows $dh/dP|_s$ versus $A_{\text{res}}^{-1/2}$ measured on I2 for five materials: stainless steel, hardened steel, an aluminum alloy, a tungsten alloy, and fused quartz. All P – h data are corrected with the same directly measured value of C_f for I2 ($0.485 \mu\text{m/N}$), and A_{res} was measured through optical image analysis at a magnification of $500\times$ (Fig. 4). As the y intercept for each data set is nearly zero ($y_{i,\text{avg}} = 0.009 \mu\text{m/N}$), these data show that direct measurement of C_f accounts for the total frame compliance with uncertainty slightly exceeding the estimate defined by the finite compliance of the sample and cyanoacrylate layer ($\pm 0.002 \mu\text{m/N}$). The variation in excess of this estimate can be attributed to uncertainties associated with the calculation of $dh/dP|_s$ via a power-law fit to a fixed portion of the unloading data as well as uncertainties in the thickness and elastic modulus of the adhesive layer. Figure 3(b) shows calculated values of E_r for each material, with and without correction for the

geometrical imperfections of the indenter relative to the ideal diamond area function $A(h_c)$. It is clear that although the average value of E_r obtained over all loads for each sample compares well with that measured independently via uniaxial compression (data not shown) and that reported in the literature for these materials, the value at a particular load can differ by as much as 22% and is consistently less than that obtained via compression. Because Fig. 3(a) indicates that C_f has been accounted for accurately, the reason for this discrepancy can be attributed unambiguously to inaccurate determination of A_{max} (i.e., assumption that $A_{\text{res}} = A_{\text{max}}$ and geometrical imperfections of the indenter). This conclusion is a clear advantage of the direct measurement approach. As Fig. 3(b) indicates, separate determination of $A_{\text{max}}(h_c)$ for fused quartz, a material for which the Oliver–Pharr assumptions of sink-in generally hold, can be applied to correct the analysis of data from a different material (316L stainless steel) via Eq. (3). The values of E_r thus determined are within 10% of compression and literature values, verifying the accuracy and utility of direct frame compliance measurement. It should be noted that the greatest discrepancy in calculated values of E_r was found for the material that showed the greatest and most anisotropic pile-up (aluminum alloy). Such extensive pile-up decreases the accuracy of empirical functions such as $A_{\text{max}}(h_c)$, despite the accuracy of directly measured values of frame compliance.

Although the instrument design used in this study is particularly amenable to direct C_f calibration, the above method is completely general and can be implemented via straightforward modifications to other commercially available indenters. The key is that the flat punch must be mounted in the load train such that the bond between this

stub and the test sample can be broken without causing damage to the load train and associated transducers. For example, the MTS NanoInstruments and Hysitron Inc. load trains could accommodate a second diamond holder mounted with a pin-nut mount, such as that used in the current study, or manufacturers could make similar, minor adjustments to the current indenter mounts such that the indenter could be retracted from the load train while remaining fixed to the sample surface.

V. CONCLUSIONS

We have presented a new method to evaluate directly the compliance of the load frame used in nano- and microindentation experiments. The chief advantages of this method are as follows:

- (1) Displacement of the instrument is actuated and measured in the same manner as during indentation experiments.
- (2) The value of C_f is not inferred from indentation data.
- (3) The method does not require estimation or direct measurement of indentation contact areas.
- (4) The method does not rely on the precision and accuracy of algorithms that convert indentation response to mechanical property values.

In addition, this method does not assume ideality of instrument deflection and can quantify effects of load, loading direction, loading rate, and load train modifications. We find that this direct measurement of C_f more accurately reflects the correction factor that must be applied to all indentation data and provides the opportunity to determine unambiguously other sources of uncertainty in the quantification of mechanical behavior through instrumented indentation experiments.

REFERENCES

1. W.C. Oliver and G.M. Pharr. *J. Mater. Res.* **7**, 1564 (1992).
2. W.D. Nix, Elastic and plastic properties of thin films on substrates: Nanoindentation techniques. *Mater. Sci. Eng. A* **234**, 37 (1997).
3. M. Dao, N. Chollacoop, K.J. Van Vliet, T.A. Venkatesh, and S. Suresh. *Acta Mater.* **49**, 3899 (2001).
4. M.F. Doerner and W.D. Nix. *J. Mater. Res.* **1**, 601 (1986).
5. T.A. Venkatesh, K.J. Van Vliet, A.E. Giannakopoulos, and S. Suresh. *Scr. Mater.* **42**, 833 (2000).
6. J. Alcala, A.E. Giannakopoulos, and S. Suresh. *J. Mater. Res.* **13**, 1390 (1998).
7. K.W. McElhaney, J.J. Vlassak, and W.D. Nix, *J. Mater. Res.* **13**, 1300 (1998).
8. G.M. Pharr and A. Bolshakov. *J. Mater. Res.* **17**, 2660 (2002).
9. A. Bolshakov and G.M. Pharr, *J. Mater. Res.* **13**, 1049 (1998).
10. J.J. Vlassak and W.D. Nix, *J. Mech. Phys. Solids* **42**, 1223 (1994).
11. M. Tansky, Elmer's Products, Inc. (private communication).